Accepted Manuscript

Title: Modulating the photocatalytic activity of TiO_2 (P25) with lanthanum and graphene oxide

Authors: Leticya Lais Coelho, Dachamir Hotza, Arthur Senra Estrella, Suélen Maria de Amorim, Gianluca Li Puma, Regina de Fatima Peralta Muniz Moreira

PII: S1010-6030(18)30821-9
DOI: https://doi.org/10.1016/j.jphotochem.2018.11.048
Reference: JPC 11620

To appear in: *Journal of Photochemistry and Photobiology A: Chemistry*

Received date: 11 June 2018
Revised date: 29 November 2018
Accepted date: 30 November 2018

Please cite this article as: Lais Coelho L, Hotza D, Senra Estrella A, de Amorim SM, Li Puma G, de Fatima Peralta Muniz Moreira R, Modulating the photocatalytic activity of TiO_2 (P25) with lanthanum and graphene oxide, *Journal of Photochemistry and amp; Photobiology, A: Chemistry* (2018), https://doi.org/10.1016/j.jphotochem.2018.11.048

This is a PDF file of an unedited manuscript that has been accepted for publication. As a service to our customers we are providing this early version of the manuscript. The manuscript will undergo copyediting, typesetting, and review of the resulting proof before it is published in its final form. Please note that during the production process errors may be discovered which could affect the content, and all legal disclaimers that apply to the journal pertain.

ACCEPTED MANUSCRIPT

Modulating the photocatalytic activity of TiO_2 (P25) with lanthanum and graphene oxide

Leticya Lais Coelho[1], Dachamir Hotza[1], Arthur Senra Estrella[1], Suélen Maria de Amorim[1], Gianluca Li Puma[2], Regina de Fatima Peralta Muniz Moreira[1,*]

[1]Laboratory of Energy and Environmental Process, Department of Chemical and Food Engineering, Federal University of Santa Catarina, Campus Universitário Trindade, 88040 900, Florianópolis, SC, Brazil

[2]Environmental Nanocatalysis & Photoreaction Engineering, Department of Chemical Engineering, Loughborough University, LE11 3TU Loughborough, United Kingdom

*Corresponding author: R.F.P.M Moreira (regina.moreira@ufsc.br)

Graphical Abstract

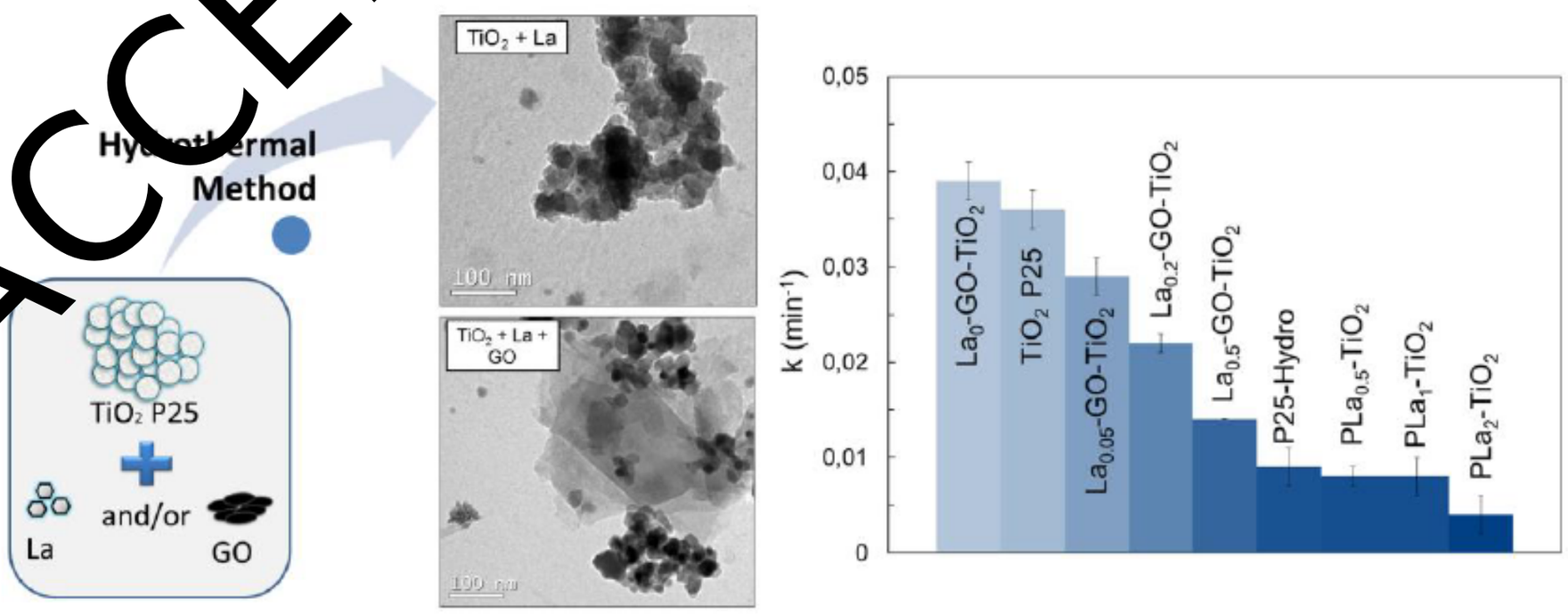

ACCEPTED MANUSCRIPT

Highlights

- The photocatalytic activity modulation concept was demonstrated.
- La-doped TiO_2 may be used as a tool for suppressing the photoactivity.
- La inhibited particle agglomeration and increased the thermal stability of anatase.
- The addition of GO reduced charge recombination and improved adsorption ability.

Abstract

The modulation and tuning of the photocatalytic activity of commercial titanium dioxide (TiO_2) P25 nanoparticles is demonstrated through the incorporation of lanthanum (La) and/or graphene oxide (GO). These composite materials, which could have applications in commercial products, were prepared by a two-step hydrothermal method from the corresponding precursors. The effect of La (0.05 - 2 mol%) and GO (5 m%) content on the crystal structure, morphology and photocatalytic activity of TiO_2 was investigated by XRS, SEM, EDS, TEM, UV-visible DRS, point of zero charge, photoluminescence and the decolorization of methylene blue. Lanthanum modified the recombination rate of the photogenerated electron-hole charges on TiO_2 by inducing an increase in the structural defects, which resulted in a significant suppression, up to 90%, of the photocatalytic activity in the UVA light region. In contrast, the addition of GO enhanced the photocatalytic activity of TiO_2. Materials with tuned intermediate photoactivity within the entire range from high to very low were prepared by dosing appropriate amounts of La and GO species. The strategy of combining La and GO represents a useful and simple method for tuning or for suppressing the photocatalytic activity of TiO_2 under UVA light irradiation in materials and consumer products using TiO_2.

ACCEPTED MANUSCRIPT

Keywords: titanium dioxide; graphene oxide; rare earths; lanthanides.

1. Introduction

The semiconductor titanium dioxide (TiO_2) has been widely investigated in recent decades as an effective photocatalyst for the decomposition of organic molecules [1]. When TiO_2 absorbs light with energy higher than its bandgap, primarily in the UV region of the electromagnetic spectrum, electron-hole pairs are created within the bulk of the solid. These photogenerated charges, after migration to the surface, can react with adsorbed O_2 and H_2O, yielding highly powerful radical oxidizing species (ROS), which in turn can decompose organic molecules into CO_2 and H_2O [2].

Extensive research efforts have been directed toward enhancing the photocatalytic activity of TiO_2; however, for some applications the activity of TiO_2 should be partially or completely suppressed. The photocatalytic activity of TiO_2 should be suppressed, for instance, when it is used in the formulation of polymers and regular paints, since this may induce a loss of their optical and mechanical properties when exposed to light irradiation. In sunscreen formulations containing TiO_2 or other semiconductor materials, the photogenerated species may cause damage to DNA and human health [3,4]. In the established application as a white pigment for paints, plastics and other products, the catalytic activity of titanium dioxide reduces the long-term durability of the polymeric materials [5].

On the other hand, TiO_2 has also been incorporated into photocatalytically active paints to impart self-cleaning and self-disinfecting properties to the painted surfaces, as well as photoactive thin film surfaces for the decontamination of air contaminants. In these cases, the photocatalytic activity of the paint or film should be partially preserved

ACCEPTED MANUSCRIPT

without affecting the durability and quality of the painted film or promoting the formation of toxic compounds resulting from the decomposition of organic additives used in the paint products [6,7]. As a consequence, the properties of such films or paints, particularly when used in an indoor environment, would need to be optimized in order to minimize the risk of the emission of harmful substances.

The total suppression of the photocatalytic activity of TiO_2 can be achieved by coating with Al_2O_3 [5] or with polydimethylsiloxane films [4]. However, it has been demonstrated that the protective $Al(OH)_3$ layer on TiO_2 nanoparticles may be damaged and leached when in contact with some ions frequently present in surface water and swimming pool water, exposing the TiO_2 nanoparticles. [8]

The photocatalytic activity of TiO_2, particularly under visible light irradiation, can be altered by ion doping, anatase-rutile phase coexisting, or p-n heterojunction formation. Among then, ion doping has been proved as an efficient approach [9–12].

However, few studies have focused on modulating and/or suppressing the photocatalytic activity of TiO_2. The strategies generally applied to reduce or tune the photoactivity of semiconductor materials include metal doping or physical coating of the photocatalysts [4,13,14].

Hybrid photocatalysts with the addition of transition metals or non-metals and, more recently, rare earths and nanocarbon compounds are a promising alternative approach to modulating the photoactivity, either increasing or inhibiting it by altering the electronic properties of the semiconductor [15–20].

With non-metal doping, the replacement of the O atoms of the TiO_2 by the added component (e.g., nitrogen, sulfur or phosphorous) may result in the hybridization of 2p orbitals from the non-metal to the 2p orbital of the semiconductor, leading to the formation of new energy levels above the valence band of the semiconductor and

ACCEPTED MANUSCRIPT

narrowing of the bandgap, consequently increasing the photoactivity of TiO_2 under visible light [21]. Among the non-metals, graphene can increase the photoactivity of photocatalysts due to, among other factors, the high mobility of charges within the graphene structure and through the formation of Ti-O-C bonds [22–27]. In contrast, the metal atoms act as a mediator between the reacting species and the semiconductor through a mechanism involving the migration of the excited electrons of the semiconductor towards the energy levels of the co-catalyst [17].

Rare-earth metal doping can also introduce structural defects in the crystals of the semiconductor, such as oxygen vacancies that can act as electron withdrawal sites, which may increase the separation efficiency of photogenerated electron-gap pairs [17]. Although Ln^{3+} ions cannot replace Ti atoms in the crystalline lattice of TiO_2, due to the difference in the ionic radius, it should be possible to substitute Ln^{3+} of the lanthanide oxide with Ti, forming Ti-O-Ln bonds [28]. As a consequence, the anatase to rutile phase transition is inhibited in Ln^{3+}-doped TiO_2 when the photocatalyst is exposed to temperatures higher than 600°C [29,30].

In this study, we demonstrate the modulation of the photoactivity of TiO_2 (P25) through the synthesis of photocatalytic composites incorporating lanthanum and graphene oxide. The composites were fully characterized and their photocatalytic activity evaluated through the degradation of the methylene blue dye, to elucidate the modulation mechanism obtained by the simultaneous presence of GO and La species. Materials with tuned intermediate photoactivity within the entire range from high to very low were prepared by dosing appropriate amounts of La and GO.

2. Experimental

ACCEPTED MANUSCRIPT

The reagents used in this study were of analytical grade. The aqueous solutions were prepared using distilled water. TiO_2 P25 (Evonik) and lanthanum nitrate hexahydrate $La(NO_3)_3.6H_2O$ (Vetec) were used as received. Graphene (Graphene Nanopowder 1-5 nm, Skyspring Nanomaterials, USA) was first oxidized by treatment with ozone for 16 h to produce graphene oxide (GO) [31]. Methylene blue (MB) $C_{16}H_{18}ClN_3S_3.H_2O$ (Lafan) was selected for the evaluation of the photocatalytic activity of the materials. Nitrogen gas (N_2) was used during the heat treatment of the photocatalysts.

2.1 Synthesis

Lanthanum and/or graphene oxide were incorporated into TiO_2 P25 nanoparticles in percentages of 0.05% to 2.0% mol/mol for La:TiO_2 and 1% m/m for GO:TiO_2.

The photocatalysts were synthesized by the two-step hydrothermal method. Initially, for the ternary composites, 2.4 g of TiO_2 P25 and the desired mass of lanthanum nitrate were suspended in 70 ml of a previously prepared ethanol/water solution (1:2). Separately, 0.12 g of GO were added to 30 ml of the same solution. Both suspensions were sonicated in an ultrasonicator (Unique, model UCS 1650) at room temperature for 2 h. The suspensions were then mixed together and sonicated for an additional 2 h to ensure complete dispersion and homogeneity. The binary composite photocatalysts were prepared in a similar manner with 2.4 g of TiO_2 P25 and the desired amount of La or GO. The solids were added together in 100 ml of the ethanol/water solution and sonicated for 4 h. The resulting suspension was then placed in a Teflon autoclave and maintained at 120 °C for 3 h, allowed to cool to room temperature under atmospheric air and dried in an oven for at least 15 h at 60 °C. The subsequent solid mass was then ground manually using a pestle and mortar, resulting in a fine powder. Subsequently, each solid was

ACCEPTED MANUSCRIPT

submitted to a further thermal treatment by heating from ambient temperature to 600 °C at a heating rate of 10 °C min^{-1} and maintaining the final temperature for 3 h. The thermal treatments were carried out in air except for the samples containing GO which were heated under a N_2 atmosphere. A pure TiO_2 control sample (TiO_2 P25-Hydro) was also prepared using the two-step synthesis method. Details of all photocatalysts used in this study are summarized in Table 1.

Table 1 – Details of photocatalysts investigated in this study.

Photocatalyst	**% La (mol/mol)**	**% GO (m/m)**
TiO_2 P25	-	-
TiO_2 P25-Hydro	-	-
La_0-GO-TiO_2	-	5
$La_{0.05}$-GO-TiO_2	0.05	5
$La_{0.2}$-GO-TiO_2	0.2	5
$La_{0.5}$-GO-TiO_2	0.5	5
$PLa_{0.5}$-TiO_2	0.5	-
PLa_2-TiO_2	2.0	-

2.2 Material characterization

The crystalline structures of the photocatalysts were determined by powder X-ray diffraction (XRD). The analysis was performed at room temperature, using a Philips X 'Pert X-ray diffractometer equipped with Cu Kα at 40 kV and 30 mA, geometry θ-2θ and λ = 1.54056 Å, with a scanning speed of 0.05 ° step/s in the 2θ range of 0º to 80°. The results were quantified using the Rietveld refinement software. The surface area was measured by the BET method in an automatic adsorptometer (Autosorb-1C Quantachrome, USA). For this analysis the samples were previously degassed at 200 °C for 4 h under vacuum.

Transmittance electron microscopy (TEM) and scanning electron microscopy (SEM) images were obtained with JEM-1011 and JEOL JSM-6390LV microscopes,

ACCEPTED MANUSCRIPT

respectively. The HRTEM patterns were obtained with a JEOL, JEM 2100 microscope equipped with a field emission electron gun and operating at 200kV. For this procedure, selected samples were dispersed in an alcohol suspension and a drop of the suspension was placed over a grid with holey-carbon film.

Energy-dispersive X-ray spectroscopy (EDS) was carried with the instrument coupled to the SEM microscope. Diffuse reflectance spectra (DRS) were obtained with a Tensor 27 spectrophotometer (Bruker) from 200 to 700 nm. Photoluminescence (PL) analysis was carried out using a Varian Eclipse spectrophotometer at room temperature with an excitation wavelength of 320 nm, and a scanning rate of 0.5 nm s^{-1}, in the range of 360 to 500 nm. The point of zero charge (pH_{pzc}) of the photocatalysts was determined on a Stabino-Nanoflex analyzer.

Electron paramagnetic resonance (EPR) measurements were recorded by a Bruker ESP 300E spectrometer (Bruker Instruments, Inc.) at 300K. The EPR parameter values were obtained by treating and simulating the experimental spectra using the Windows software programs Win-EPR and SimFonia and the Weak Pitch Bruker pattern.

2.3 Photocatalytic Activity

The photocatalytic activity of the materials was evaluated in a reaction vessel (13 cm diameter) fitted with a magnetic stirring bar and a UV-A lamp ($\lambda = 365$ nm; 8W; F8T5 Blacklight blue, Ushio) positioned horizontally, 8 cm above the bottom of the reaction vessel (Fig. 1). The whole apparatus was enclosed in a black box for safety purposes and to eliminate external light interferences. In a typical photocatalytic reaction, 0.125 g of the photocatalyst was suspended in 250 mL of MB solution (10 mg L^{-1}) inside a circular vessel and mixed under strong magnetic stirring in the dark for 15 min. The reaction was initiated when the light was turned on. At regular time intervals a 3 mL aliquot of the

ACCEPTED MANUSCRIPT

suspension was collected and centrifuged or filtered through a 0.22 μm PVDF membrane (Millipore) to separate the solids. The MB concentration was measured using a HACH spectrophotometer (model DR 5000) at the wavelength of maximum absorbance ($\lambda = 665$ nm). The kinetics of MB degradation in the absence of a catalyst and under dark conditions was also investigated. All experiments were performed at pH 5.5.

Figure 1 - Experimental apparatus used for the evaluation of the photocatalytic activity of the samples.

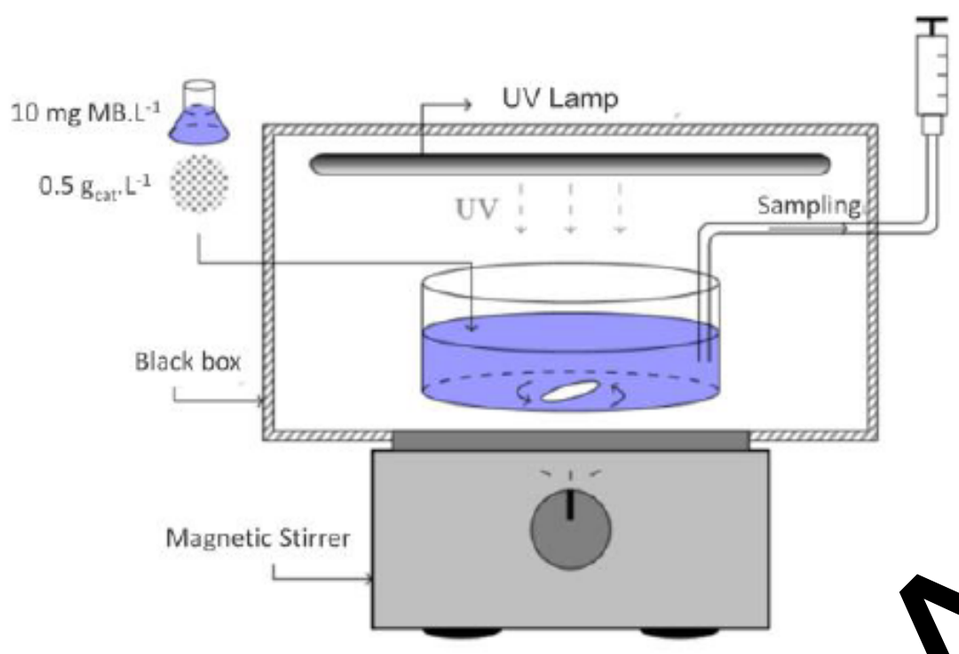

MANUSCRIPT

ACCEPTED

3. Results and Discussion

3.1 Characterization of the photocatalysts

Anatase and rutile were the only crystalline phases identified in the solid samples by XRD, which may result from the low amounts of La and GO used. The quantitative analysis (Table 2) clearly showed that the thermal treatment led to a partial anatase to rutile phase transition for the La_0-GO-TiO_2 composite sample and the P25-Hydro photocatalyst, with the percentage of rutile increasing from 14.2% in the P25 sample to 27.4% and 23.1%, respectively, in these photocatalysts. On the other hand, the stabilization of the anatase phase by La doping was observed even at low La concentrations and in the presence of graphene oxide. The amounts of rutile and anatase

ACCEPTED MANUSCRIPT

in the $La_{0.05}$-GO-TiO_2 and $La_{0.2}$-GO-TiO_2 samples were approximately equal to the values obtained for the commercial TiO_2 P25.

Because of this phase stabilization, the BET surface areas of La-doped TiO_2 samples are nearly the same, as well as the N_2 adsorption/desorption isotherms at 77 K (Figure S1). An increase in the surface area of the photocatalyst containing GO in relation to P25-Hydro was observed, which was attributed to the high surface area of the graphene (710 m^2 g^{-1}) and larger open structure. The BET surface area of ternary composite materials increased at higher lanthanum content because of the progressive stabilizing effect of lanthanum on the TiO_2-GO structure, which probably inhibits the agglomeration of the particles.

Table 2 - Quantitative XRD analysis and BET for different photocatalysts.

Photocatalyst	**Rutile (% m/m)**	**Anatase (% m/m)**	**BET surface area (m^2 g^{-1})**
TiO_2 P25	14.2	85.8	50.0
TiO_2 P25-Hydro	23.1	76.9	23.8
La_0-GO-TiO_2	27.4	72.6	46.7
$La_{0.05}$-GO-TiO_2	14.8	85.2	54.8
$La_{0.2}$-GO-TiO_2	13.6	86.4	56.7
$La_{0.5}$-GO-TiO_2	-	-	70.2
$PLa_{0.5}$-TiO_2	16.9	83.1	47.3
PLa_2-TiO_2	16.9	83.1	50.0

Figure 2 provides the SEM images for the P25-Hydro, La_0-GO-TiO_2 and PLa_2-TiO_2 materials. The particles show an agglomerated and irregular morphology and size. This characteristic was common to all photocatalysts and structural changes were not identified in any of the samples. The presence of La and GO on the surface of the photocatalyst was not noted, due to the very small particle size and/or the low amount used, indicating a high degree of dispersion in the samples.

ACCEPTED MANUSCRIPT

ACCEPTED MANUSCRIPT

ACCEPTED MANUSCRIPT

ACCEPTED MANUSCRIPT

Figure 2 - SEM images of (a) TiO_2 P25-Hydro, (b) La_0-GO-TiO_2 and (c) PLa_2-TiO_2.

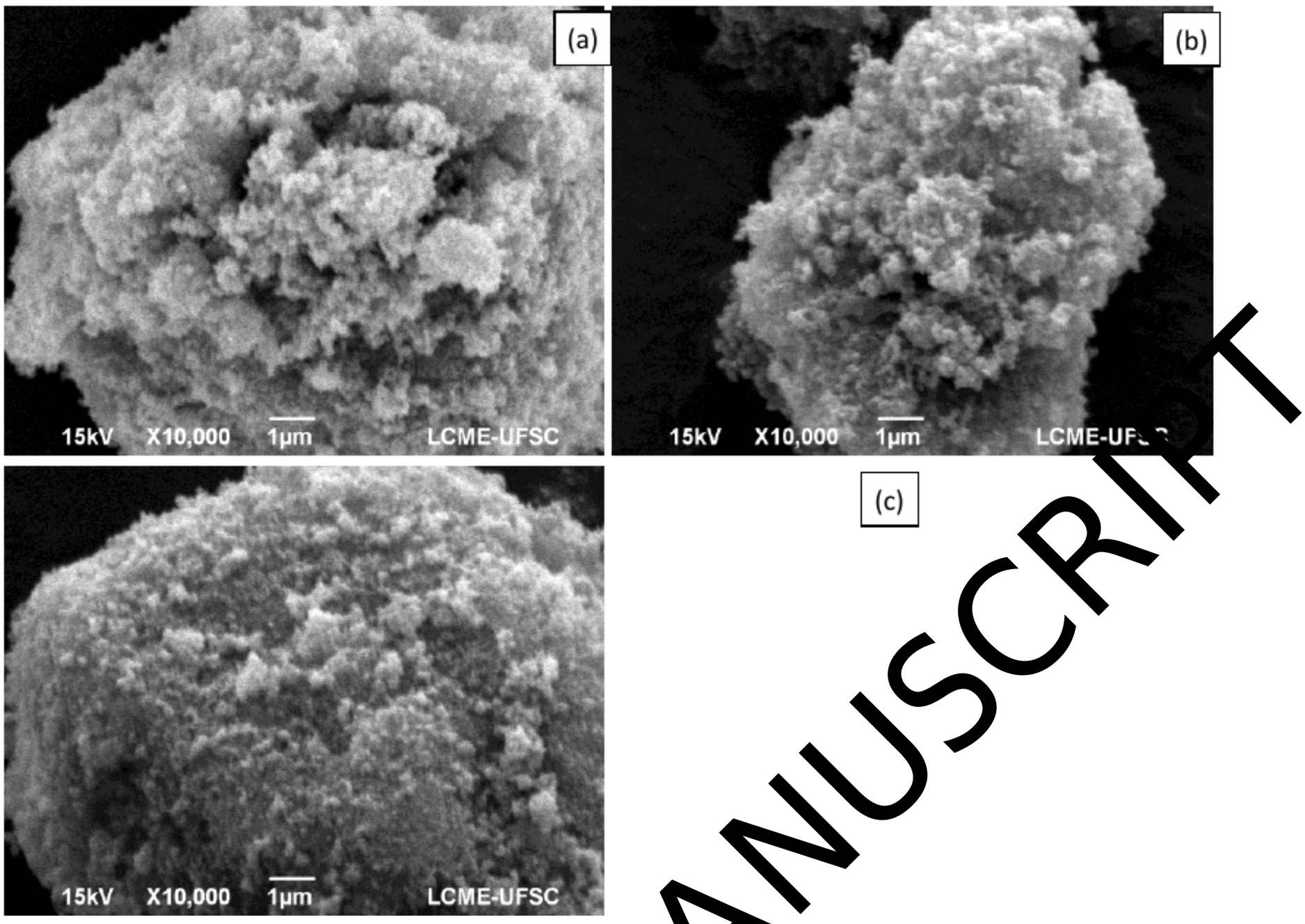

Furthermore, the semi-quantitative analysis of EDS by area (Figs. 3 and 4) showed the presence of carbon originating from GO and lanthanum on the surface of the La_0-GO-TiO_2, $La_{0.5}$-GO-TiO_2 and PLa_2-TiO_2 composites (Table 3). Small differences were observed in the results, which was attributed to the nominal amounts of each compound added during the doping procedure. This verified the good degree of dispersion of the graphene oxide and lanthanum in the photocatalysts.

ACCEPTED MANUSCRIPT

ACCEPTED MANUSCRIPT

Figure 3 - SEM images and EDS areas for (a) La_0-GO-TiO_2, (b) $La_{0.5}$-GO-TiO_2 and (c) PLa_2-TiO_2.

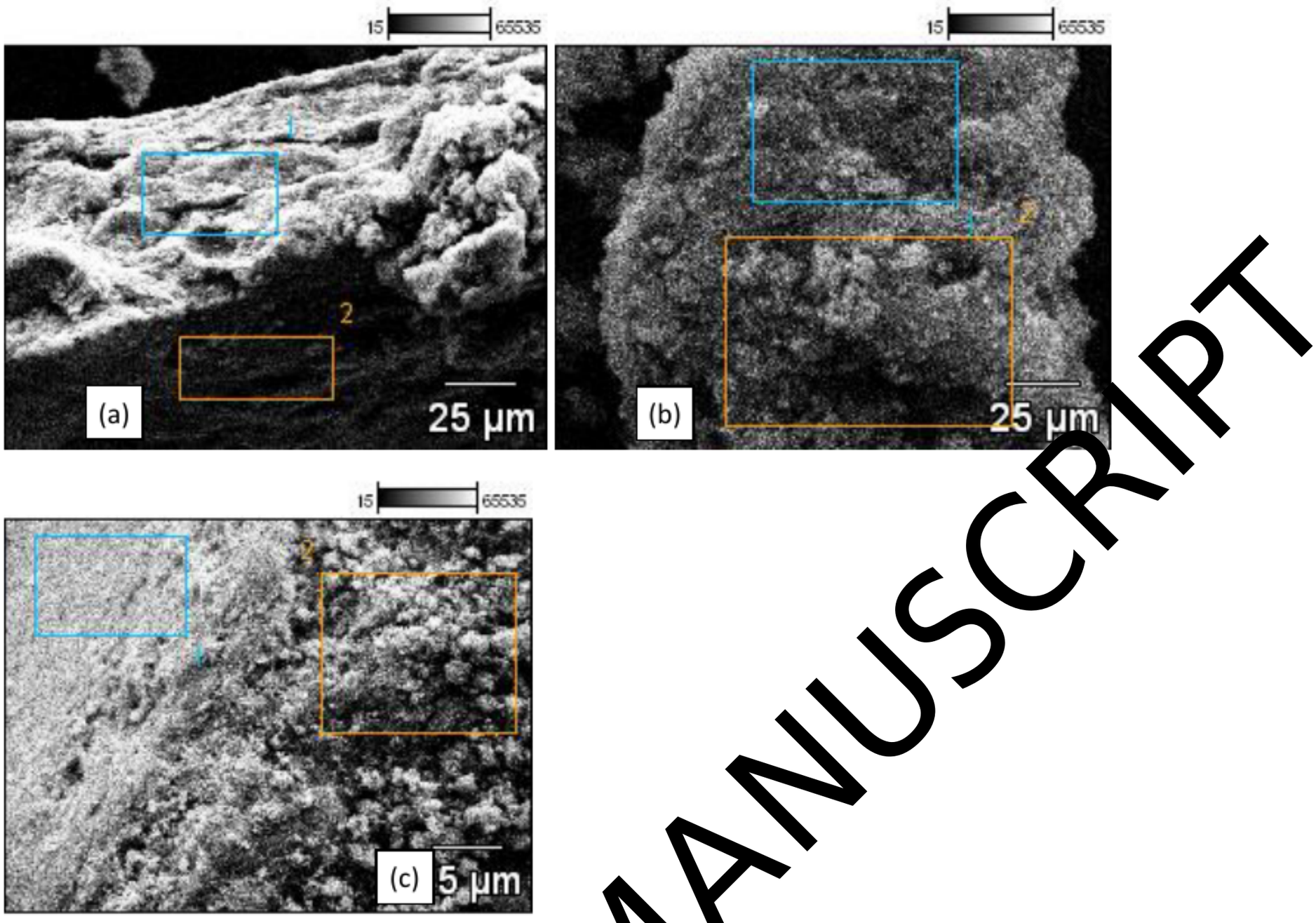

Table 3 - Semi-quantitative analysis of EDS results by area*.

Composite	C (m%)	La (mol%)
	area 1 - area 2	area 1 - area 2
La_0-GO-TiO_2	4.44 – 8.02	0
$La_{0.5}$-GO-TiO_2	4.42 – 3.09	0.30 – 0.31
PLa_2-TiO_2	0	1.62 – 2.19

*Areas 1 and 2, according to Fig. 3.

The TEM images showed very similar structures for TiO_2 P25 (Fig. 4a) and P25-Hydro (Fig. 4b) with well-defined contours, although the latter appears to be slightly more agglomerated. Therefore, it was considered that any structural or morphological modifications of the composite photocatalysts could be attributed to the presence of lanthanum and/or graphene oxide. The image for $La_{0.5}$-GO-TiO_2 clearly shows TiO_2

ACCEPTED MANUSCRIPT

particles adhered to the graphene sheets (Fig. 4c). The small particles of La_2O_3 were difficult to visualize by TEM due to their morphological similarity with TiO_2. However, even in the visual absence of lanthanum hydroxide needles, the presence of lanthanum was indicated by the surface modifications observed on the samples with La, which were characterized by a loss of well-defined contours, as shown in Fig. 4d for $La_{0.5}$-GO-TiO_2 and Fig. 4e for PLa_2-TiO_2. No regions were identified on the images where the presence of titanium, lanthanum and graphene was visible. This demonstrates a low degree of homogeneity of the samples, as well as a possible lack of affinity between the carbon and lanthanum compounds.

Lanthanum atoms are unable to enter the crystalline network of TiO_2 due to their large atomic radius [32] and, as a result, will remain on the surface of the photocatalyst. The surface coating of TiO_2 with lanthanum oxide could be responsible for the formation of recombination sites (as confirmed by the photoluminescence analysis, Fig. 7), with a consequent decrease in the photocatalytic activity. Despite the good dispersion of graphene oxide and lanthanum suggested by the EDS results (Table 3), TiO_2 agglomerates without surface modifications were also found in the photocatalytic composites.

ACCEPTED MANUSCRIPT

ACCEPTED MANUSCRIPT

Figure 4 - TEM images for P25 (a), P25-Hydro (b), $La_{0.5}$-GO-TiO_2 (c-d) and PLa_2-TiO_2 (e).

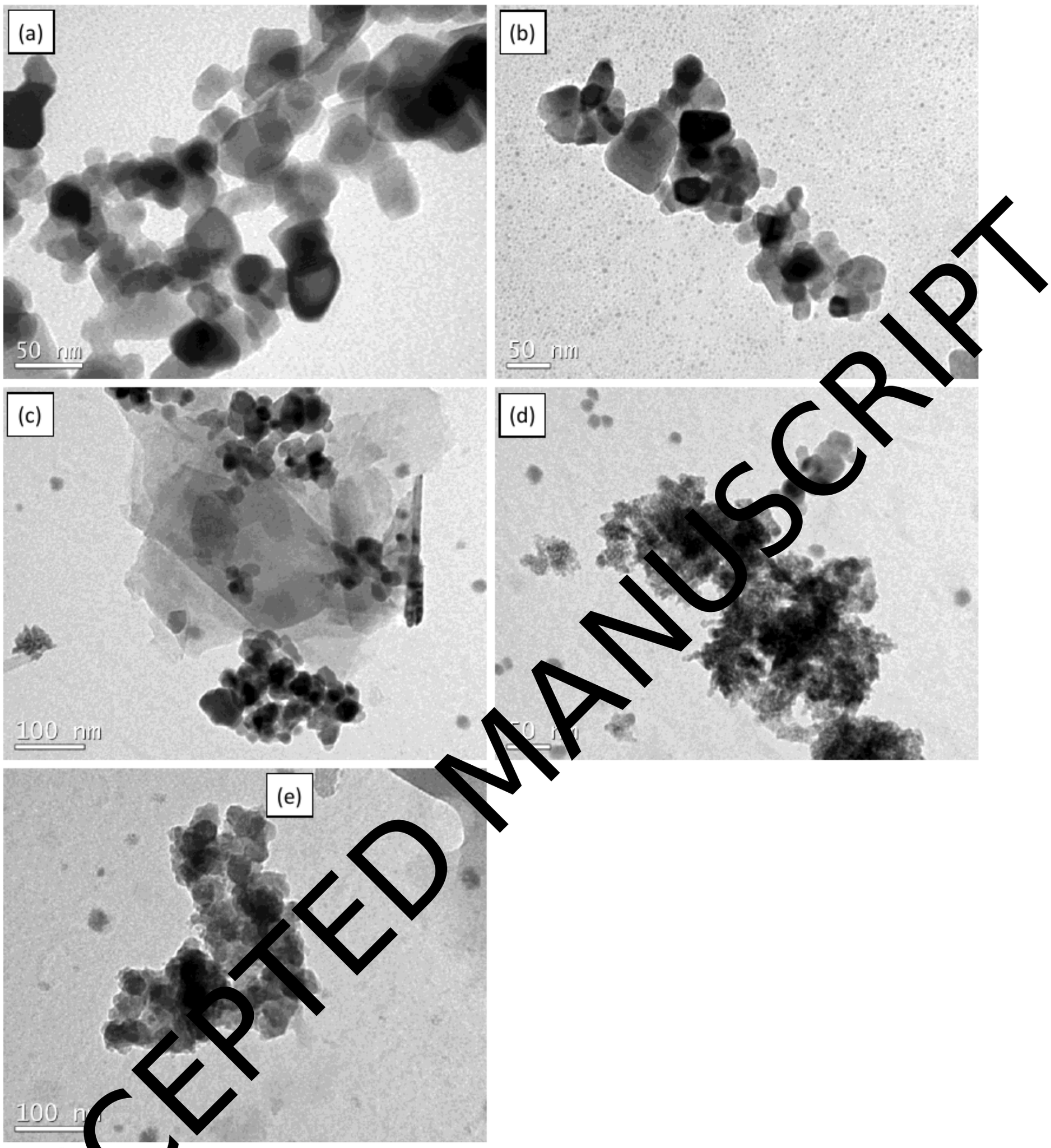

The HRTEM results are shown in Figure 5. The interlayer spacings d = 0.33 nm and d = 0.17 nm of the La_2-TiO_2 sample correspond to the (1 0 1) and (2 1 1) planes of anatase, respectively (Fig.5d). Moreover, there is no lattice distortion in the nanoparticles, and all atoms are well-aligned in the lattice. The fringes of doped anatase lattice (La_2-

ACCEPTED MANUSCRIPT

TiO_2) do not appear to be expanded, but showed waviness (see Fig. 5c), which could be ascribed to possible electric stress originating from the La ion doping [33].

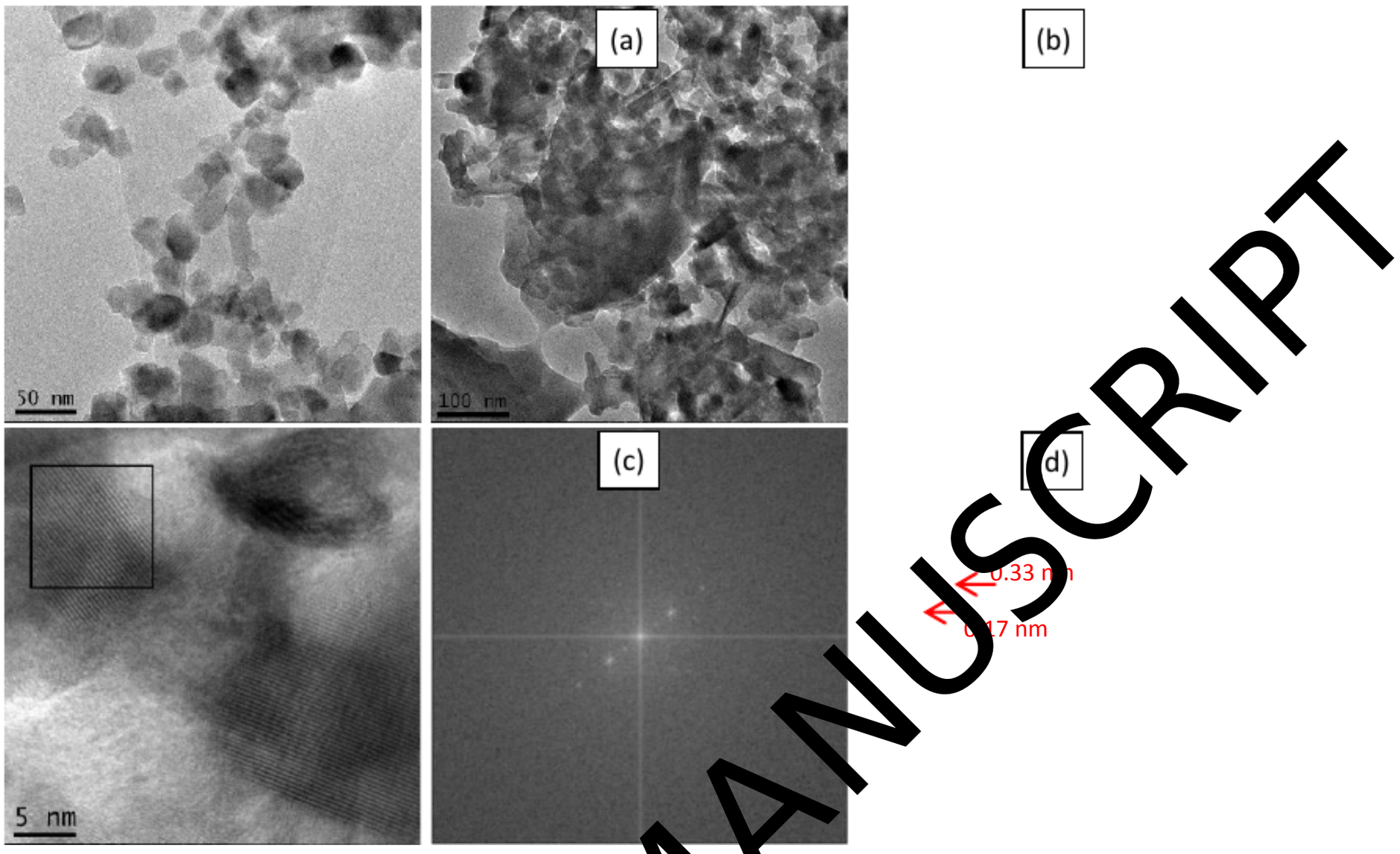

Figure 5: HRTEM micrographs of selected samples: (a) $La_{0.5}$-GO-TiO_2 ;(b) and (c) La_2-TiO_2; (d) SAED pattern of La_2-TiO_2.

The DRS spectra are presented in Figure 6. All photocatalysts showed a high degree of absorption and a similar absorption behavior as TiO_2 [34] up to the beginning of the UV-A region (315 to 400 nm), after which significant differences were noted. The materials with GO showed high absorption in the visible region, which decreased slightly with increasing amounts of lanthanum, from 0 to 0.5%. All composites containing GO are greyish, so it is expected that the high absorption of these photocatalysts is due to the presence of GO [35]. According to previous reports [31,36], chemical Ti-O-C bonds were formed when the photocatalysts were prepared under the same experimental conditions.

Figure 6 – DRS spectra (a) and Kubelka-Munk function ($F_{KM}\, h\nu^{1/2}$) (b) for different photocatalysts.

ACCEPTED MANUSCRIPT

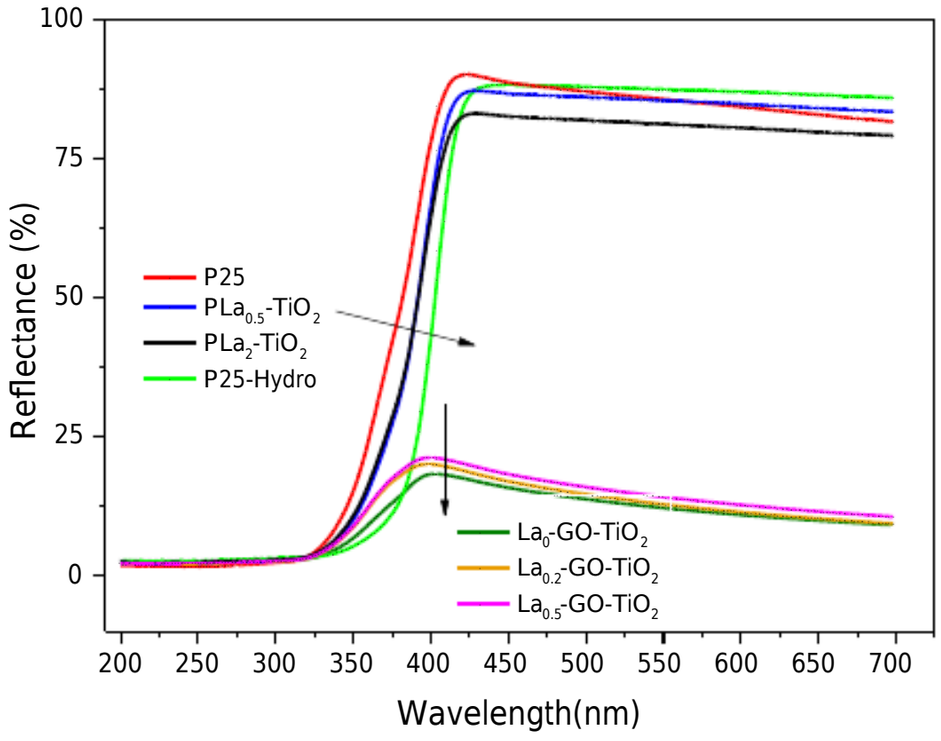

(a)

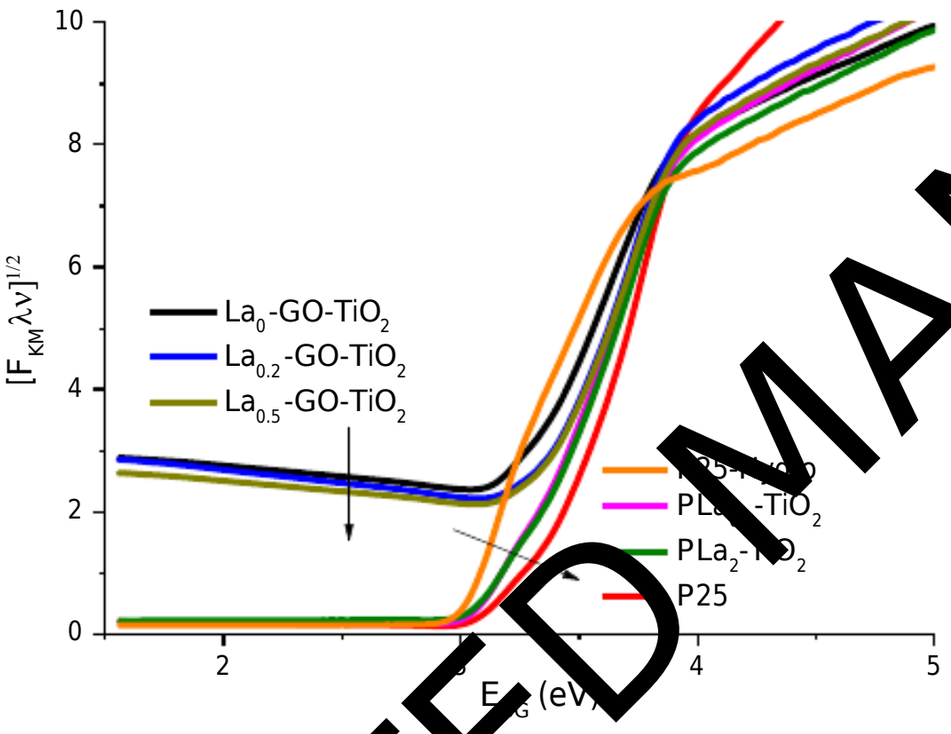

(b)

In contrast the TiO_2 with La, which does not change the final color of the composite, showed low absorption in the visible range, similar to TiO_2 P25, although PLa_2-TiO_2 had a slightly higher absorption in the visible region. The reflectance data were used to estimate the bandgap energy (Table 3) from the Kubelka-Munk function ($F_{KM}(RD)$) (Equation 1).

$$\frac{(\quad)^2}{2RD} \quad \frac{\quad}{s} \qquad (1)$$

ACCEPTED MANUSCRIPT

where S is the scattering factor, is the molar extinction coefficient, $h\nu$ is the photon energy and RD is the diffuse reflectance.

As seen in Table 4, TiO_2 P25-Hydro and La_0-GO-TiO_2 were the photocatalysts with the lowest bandgap values (2.85 and 3.05 eV). All other photocatalysts had bandgap energies varying between 3.16 and 3.36 eV (Table 4). This narrowing of the bandgap is usually attributed to the formation of Ti-O-D bonds where D is a generic substance, such as Ti-O-C when graphene oxide is added to the TiO_2. This suggests that the addition of a metal and/or non-metal can play a fundamental role in the absorption of visible light, resulting in a modification of the fundamental process of the formation of photogenerated charge carriers, with bandgap narrowing of TiO_2 obtained by either increasing the valence band and/or by decreasing the conduction band [37].

Table 4 – Bandgap energy (E_{BG}) for different photocatalysts.

Photocatalyst	**E_{BG} (eV)**
TiO_2 P25	3.36
P25-Hydro	2.85
La_0-GO-TiO_2	3.05
$La_{0,2}$-GO-TiO_2	3.16
$La_{0,5}$-GO-TiO_2	3.16
$PLa_{0,5}$-TiO_2	3.20
PLa_2-TiO_2	3.22

The photoluminescence results (Fig. 7) showed an increase in the emission intensity in the region of 365 to 393 nm, which was correlated to the La and/or GO content. This region corresponded approximately to the bandgap energies of the photocatalysts [38]. The PL emission intensity of the samples with La were considerably higher, in comparison to the value for P25-Hydro, as a result of an increase in the surface oxygen

ACCEPTED MANUSCRIPT

vacancies and structural defects acting as recombination centers. However, a La content in the range of 0.5 to 2.0% did not appear to change the intensity of the PL spectra.

Figure 7 - Photoluminescence results for different photocatalysts.

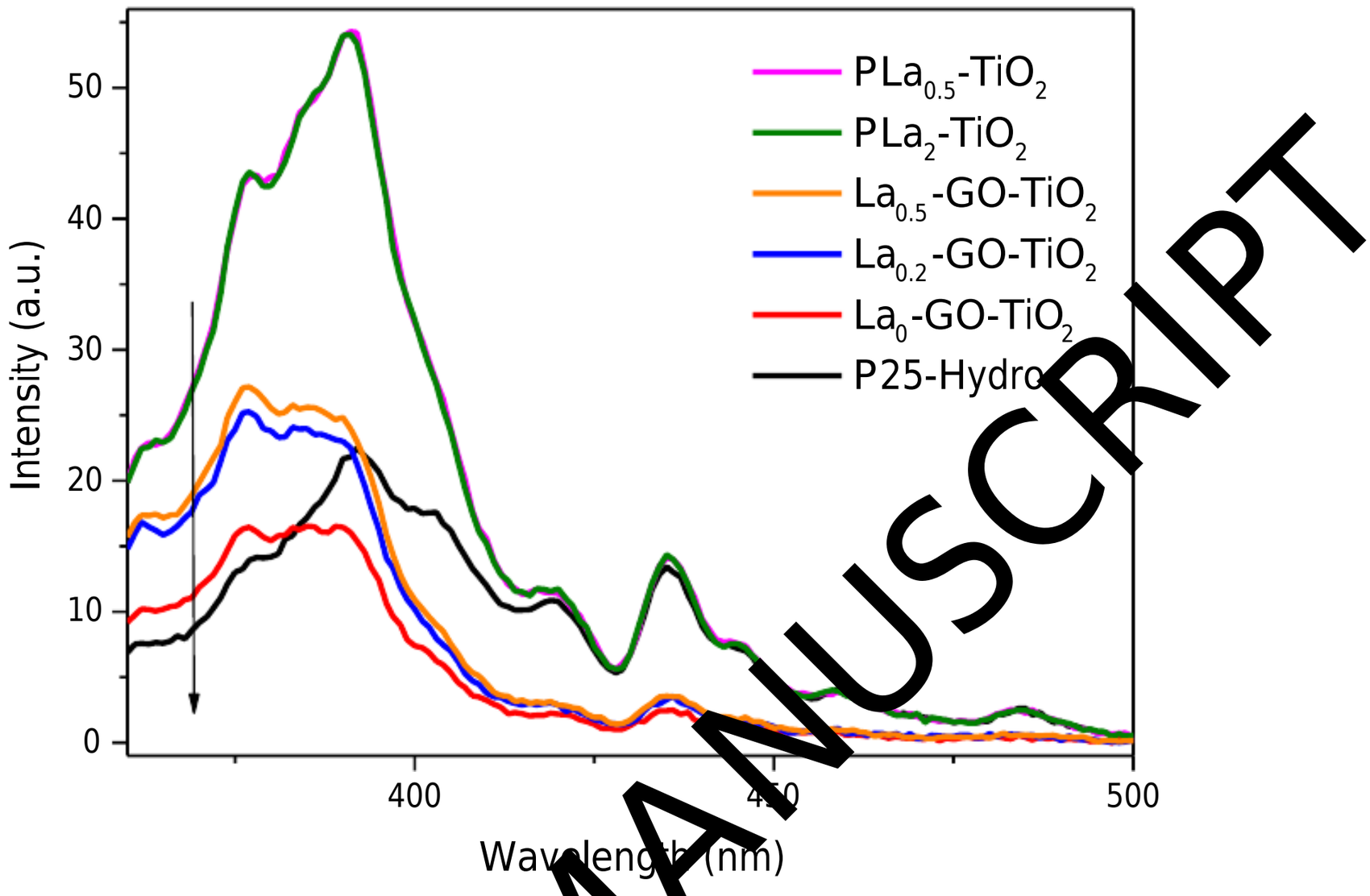

The introduction of GO in the sample with La resulted in a marked reduction in the PL emission intensity. This phenomenon is well known and attributed to the high electronic conductivity of GO, which reduces the charge recombination. In the visible region, the ternary composites had the same profile as the samples with GO, presenting almost negligible emission. Since the samples with GO absorb considerably more radiation in the visible region than the P25-Hydro sample, this low emission intensity is indicative of higher photocatalytic activity in the visible light region.

EPR spectroscopy was used to detect the generated paramagnetic species and thus identify various trap sites for photogenerated electrons and holes. The spectra of $La_{0.5}$-GO-TiO_2, La_0-GO-TiO_2 and $PLa_{0.5}$-TiO_2 exhibited similar lineshapes (Figure S2), and $La_{0.5}$-GO-TiO_2 showed clearer spectrum than La_0-GO-TiO_2 or $PLa_{0.5}$-TiO_2. The *g*-values

ACCEPTED MANUSCRIPT

found in this work are in the range reported in the literature and suggested that the as samples generated radicals such as $O^{\bullet-}$, $O_2^{\bullet-}$, $Ti^{4+}O_3^{\bullet-}$, $Ti^{4+}O^{\bullet-}$, and $Ti^{4+}OH^{\bullet-}$, as well as oxygen vacancies ($V_o^{\bullet}$). [39-41]

The signal corresponding to g ~ 2.03 should be ascribed to oxygen-centered anion radical covalently bound to titanium atoms in the of $Ti^{4+}O^{2-}Ti^{4+}O^{\bullet-}$ species on the surface produced by surface brindging oxygen atoms trapping photogenerated holes, as proposed by Hongquan et al. [42].. This oxygen-centered anion radical is known to be responsible for most of the primary oxidation processes [39, 42, 43]. The EPR signal at about g ~ 1.96 – 1.98 could indicates the formation of Ti^{3+} species at surface sites, and the signal with g ~ 2.002 - 2.003 is due to the presence of oxygen vacancies [39, 40, 44, 45]. The appearance of Ti^{3+} into TiO_2 has been explained to the formation of cross-linked bond Ti^{4+}–O–M^{3+} (M is a metal), which coexists with oxygen vacancies [43]. So, the formation of Ti–O–La bonds could explain the EPR signals measured for lanthanum doped-TiO_2 samples (Figure S2a and Figure S2c) [46, 47].

3.2 Photocatalytic activity

Table 5 shows the amount of MB adsorbed over the photocatalysts in the dark prior to irradiation and the point of zero charge of the respective photocatalysts. The samples with CO presented a higher adsorption capacity as a result of their larger surface area. In contrast, the samples containing lanthanum strongly inhibited the adsorption of MB since the addition of lanthanum caused an increase in the point of zero charge of the solids. The surface charge of the La-TiO_2 composite is positive at the pH used in the experiments, causing repulsion effects regarding the adsorption of the cationic dye (MB). This effect became stronger as the amount of lanthanum in the solid increased.

ACCEPTED MANUSCRIPT

Table 5 - Methylene blue adsorbed by the photocatalysts in the dark and the point of zero charge.

Photocatalyst	**MB adsorbed (%)**	**pH_{pzc}**
TiO_2 P25	15.2	6.2
P25-Hydro	11.5	4.9
La_0-GO-TiO_2	32.0	5.3
$La_{0.05}$-GO-TiO_2	26.4	-
$La_{0.2}$-GO-TiO_2	19.0	-
$La_{0.5}$-GO-TiO_2	19.7	5.7
$PLa_{0.5}$-TiO_2	1.7	-
PLa_1-TiO_2	5.4	-
PLa_2-TiO_2	1.4	7.8

With regard to the decolorization of MB under UV light irradiation, in the absence of a photocatalyst it was insignificant but in the presence of a photocatalyst the decolorization followed pseudo-first-order kinetics (Fig. 8) for all materials investigated.

ACCEPTED MANUSCRIPT

ACCEPTED MANUSCRIPT

Figure 8 - Kinetics of MB decolorization using different photocatalysts under UVA irradiation.

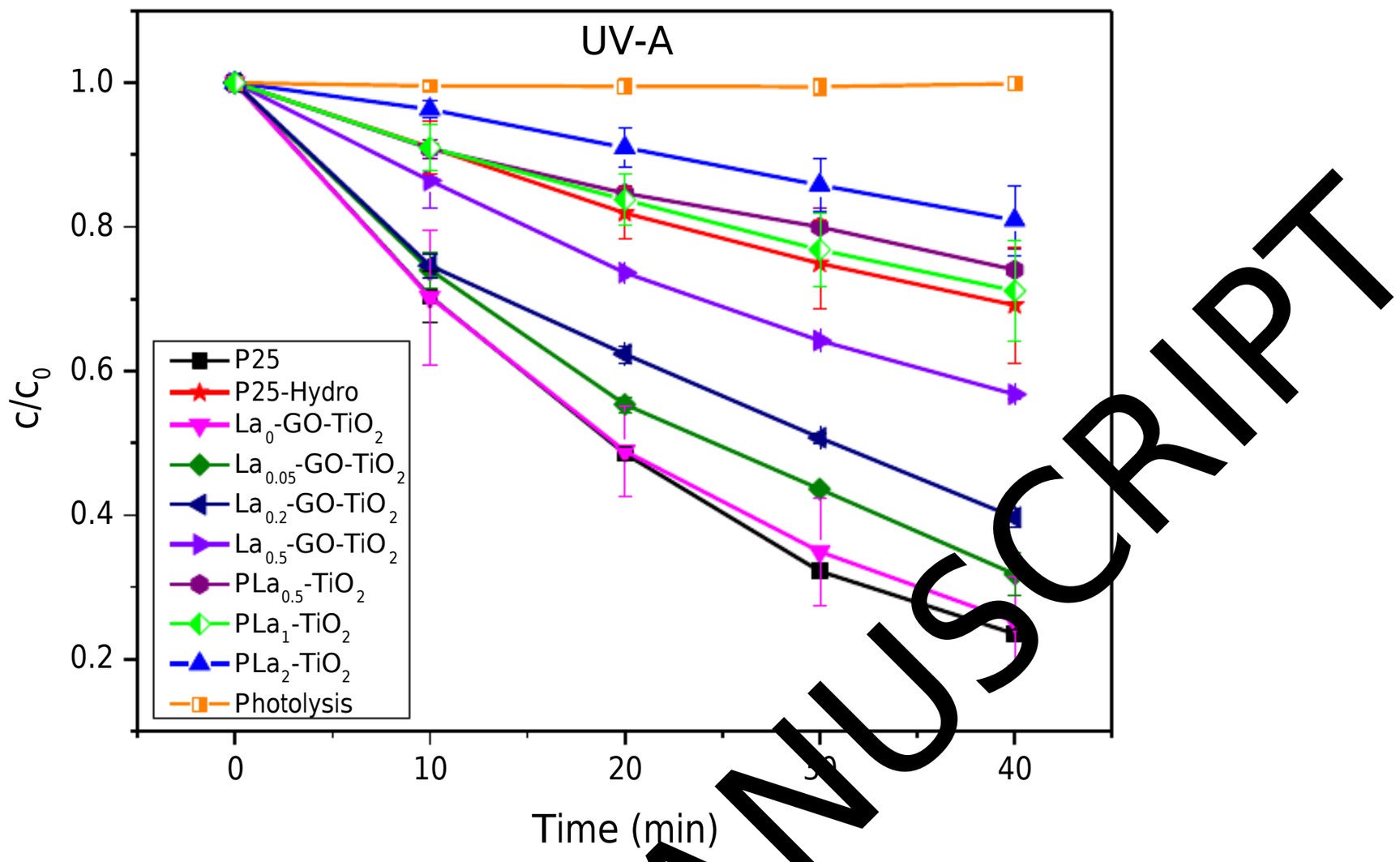

The reaction kinetics constants obtained from fitting the experimental data to the material balance equation for the batch reactor combined with first-order reaction kinetics (Eq. 2) are shown in Table 6.

— (2)

ACCEPTED MANUSCRIPT

Table 6 - Pseudo-first-order kinetics constants for MB decolorization using different photocatalysts under UVA irradiation.

Photocatalyst	**k (min^{-1})**	**R^2**
TiO_2 P25	0.036 ±0.002	0.997
P25-Hydro	0.009 ±0.002	0.994
La_0-GO-TiO_2	0.039 ±0.001	0.999
$La_{0.05}$-GO-TiO_2	0.029 ±0.002	0.992
$La_{0.2}$-GO-TiO_2	0.022 ±0.001	0.992
$La_{0.5}$-GO-TiO_2	0.014 ±0.000	0.993
P$La_{0.5}$-TiO_2	0.008 ±0.001	0.978
PLa_1-TiO_2	0.008 ±0.002	0.997
PLa_2-TiO_2	0.004 ±0.002	0.997

The incorporation of lanthanum in TiO_2 produced a strong suppression effect on the decolorization rate, which increased with higher amounts of La. Several authors have reported an enhanced photocatalytic activity of TiO_2 with the addition of lanthanides and this has generally been attributed, among other factors, to a higher electronic mobility of the photogenerated charges and consequent decrease in their recombination rate. However, the nanocomposites prepared in this study expressed elevated rates of charge recombination, as shown by the PL results, which suppressed the photocatalytic activity, as expected based on the chemical and physical characteristics obtained. The positive effect of lanthanides on photoactivity is generally obtained up to an optimum amount and a negative effect is due to the formation of recombination centers for photogenerated e^-/h^+ pairs [40].

The increase in photoactivity in the visible range of the spectrum for the La-TiO_2 composite results from the modification of the electronic structure of TiO_2. However, this phenomenon is often accompanied by a marked decrease in the photoactivity of the

ACCEPTED MANUSCRIPT

catalyst in the UV region [49, 50]. The amount of La^{3+} necessary to achieve the highest photoactivity under visible light irradiation may promote an excessive increase in the Ti^{3+} species, which acts as a photo-hole trap under UV light irradiation. Therefore, the optimum amount of La^{3+} is related to the amount of Ti^{3+} species acting as charge-carrier combination centers. This optimum amount of La^{3+} could be as low as 0.25 mol% [49], while higher contents of La^{3+} would reduce the photocatalytic activity of TiO_2, especially under UV irradiation. Below this low concentration, photoelectrons and photo-holes have the slowest recombination rate and this produces the highest quantum yield for the photocatalytic process.

However, when GO and La are simultaneously added in TiO_2, the suppressing effect is also noted even at very low La^{3+} contents (0.05 mol%, Figure 7), indicating that La^{3+} may provide a safer and more efficient way to modulate the photocatalytic activity of TiO_2 in consumer products, such as sunscreens, powders and pigments, where the total suppression is not desirable.

Although there is a shift in the absorption band, meaning that more photons can be absorbed in the visible region, the photocatalytic activity may decrease since the addition of other substances (such lanthanides) to TiO_2 also generates structural defects on the surface of the photocatalyst, such as oxygen vacancies. Depending on their quantity, these can act as sites of charge recombination, leading to suppression of the photoactivity, as observed in this study. The presence of GO in the photocatalysts led to a slight increase in the photocatalytic activity. This effect can also be attributed to the higher surface area, even after heat treatment, and to the high adsorption capacity of graphene oxide, which is essential for photocatalytic reactions. Due to the antagonistic effects of La and GO, the ternary composite photocatalysts showed intermediate photocatalytic properties. The lower photocatalytic activity observed for the P25-Hydro

ACCEPTED MANUSCRIPT

sample in comparison to pristine TiO_2 P25 can be attributed to the marked decrease in surface area caused by the thermal treatment (Table 2).

The high visible light absorption and low PL emission, with stable photoactivity in the UV region of the TiO_2-GO composites, indicates that this material may exhibit high efficiency under the full solar irradiation spectrum. Conversely, the presence of La was effective in suppressing the photocatalytic activity under UV light irradiation, without altering the adsorption or charge transportation profile in the visible region of the solar spectrum. Consequently, an increase in the photocatalytic activity under visible light irradiation generated by the metal addition, at the concentrations studied, is not expected for the La-TiO_2 composites. This suggests that these materials are potentially excellent UV light absorbers for use in applications such as sunscreens or photocatalytic paints and in other cases where photocatalytic activity is not desirable across the entire spectrum of solar light.

4. Conclusions

Lanthanum-TiO_2-graphene oxide composites were synthetized using a two-step hydrothermal method and the results showed antagonistic effects between La and GO. Lanthanum did not influence the absorption spectrum of TiO_2, however it produced electron-hole pair recombination centers, which effectively inhibited the photocatalytic activity of TiO_2, even at low concentrations. In addition, the rare earth inhibited particle agglomeration and increased the thermal stability of anatase. The photocatalytic activity of TiO_2 in the presence of GO slightly increases, due to the larger surface area of the composite and the high adsorption capacity of graphene oxide, which is essential for photocatalytic reactions. While most previously reported studies indicate an increase in TiO_2 photoactivity following the incorporation of rare earths and carbonaceous materials,

ACCEPTED MANUSCRIPT

the results reported herein show that the incorporation of La and/or GO could be useful for the modulation and tuning of the photocatalytic activity for different commercial applications.

Acknowledgments

The authors gratefully acknowledge the Brazilian funding agencies CAPES and CNPq (Grant 405892/2013-6 and 304397/2010-5) for financial support and the Central Laboratory of Electron Microscopy (LCME) of the Federal University of Santa Catarina for the SEM and TEM analyses. To Juliana Shultz for EPR measurements.

References

[1] J. Wen, X. Li, W. Liu, Y. Fang, J. Xie, Y. Xu, Photocatalysis fundamentals and surface modification of TiO_2 nanomaterials, Chinese J. Catal. 36 (2015) 2049–2070. doi:10.1016/S1872-2067(15)60999-8.

[2] M.R.. HOFFMANN, S.T.. MARTIN, W.. CHOI, D.W. BAHNEMANN, Preparation of highly stable superhydrophobic TiO_2 surfaces with completely suppressed photocatalytic activity, Chem. Rev. 95 (1995) 69–96. doi:10.1021/cr00033a004.

[3] J.F. de Lima, O.A. Serra, Cerium phosphate nanoparticles with low photocatalytic activity for UV light absorption application in photoprotection, Dye. Pigment. 97 (2013) 291–296. doi:10.1016/j.dyepig.2012.12.020.

[4] K. Kim, H. Ook, C. Won, M. Jeong, Y. Dok, D. Chan, Preparation of highly stable superhydrophobic TiO_2 surfaces with completely suppressed photocatalytic activity, Prog. Org. Coatings. 76 (2013) 596–600. doi:10.1016/j.porgcoat.2012.11.010.

ACCEPTED MANUSCRIPT

[5] U. Gesenhues, Al-doped TiO_2 pigments: influence of doping on the photocatalytic degradation of alkyd resins, J. Photochem. Photobiol. A Chem. 139 (2001) 243–251. doi:10.1016/S1010-6030(00)00429-9.

[6] R.A.R. Monteiro, A.M.T. Silva, J.R.M. Ângelo, G. V Silva, A.M. Mendes, R.A.R. Boaventura, et al., Photocatalytic oxidation of gaseous perchloroethylene over TiO_2 based paint, J. Photochem. Photobiol. A Chem. 311 (2015) 41–52.

[7] O. Geiss, J. Barrero-Moreno, C. Cacho, D. Kotzias, Photocatalytic degradation of organic paint constituents-formation of carbonyls, Build. Environ. 48 (2012) 107–112. doi:10.1016/j.buildenv.2011.08.021.

[8] J. Virkutyte, S.R. Al-Abed, D.D. Dionysiou, Depletion of the protective aluminum hydroxide coating in TiO_2-based sunscreens by swimming pool water ingredients, Chem. Eng. J. 191 (2012) 95–103. doi:10.1016/j.cej.2012.02.074.

[9] X. Sun, C. Li, L. Ruan, Z. Peng, J. Zhang, J. Zhao, et al., Ce-doped SiO_2@TiO_2 nanocomposite as an effective visible light photocatalyst, J. Alloys Compd. 585 (2014) 800–804. doi:10.1016/j.jallcom.2013.10.034.

[10] N.R. Khalid, E. Ahmed, Z. Hong, M. Ahmad, Synthesis and photocatalytic properties of visible light responsive La/TiO_2-graphene composites, Appl. Surf. Sci. 263 (2012) 254–259. doi:10.1016/j.apsusc.2012.09.039.

[11] L. Pan, X. Zhang, L. Wang, J. Zou, Controlling surface and interface of TiO_2 toward highly efficient photocatalysis, (2015) 1–5. doi: 10.1016/j.matlet.2015.06.109.

[12] M. Yasmina, K. Mourad, S.H. Mohammed, C. Khaoula, Treatment heterogeneous photocatalysis; Factors influencing the photocatalytic degradation by TiO_2, Energy Procedia. 50 (2014) 559–566. doi:10.1016/j.egypro.2014.06.068.

[13] T.H. Le, A.T. Bui, T.K. Le, The effect of Fe doping on the suppression of

ACCEPTED MANUSCRIPT

photocatalytic activity of ZnO nanopowder for the application in sunscreens, Powder Technol. 268 (2014) 173–176. doi:10.1016/j.powtec.2014.08.043.

[14] D.V. Dao, M. van den Bremt, Z. Koeller, T.K. Le, Effect of metal ion doping on the optical properties and the deactivation of photocatalytic activity of ZnO nanopowder for application in sunscreens, Powder Technol. 288 (2016) 366–370. doi:10.1016/j.powtec.2015.11.030.

[15] U. Diebold, The surface science of titanium dioxide, Surface Science Reports 48 (2003) 53-229.

[16] M.A. Henderson, A surface science perspective on TiO_2 photocatalysis, Surf. Sci. Rep. 66 (2011) 185–297. doi:10.1016/j.surfrep.2011.01.001.

[17] R. Marschall, L. Wang, Non-metal doping of transition metal oxides for visible-light photocatalysis, Catal. Today 225 (2014) 111–135. doi:10.1016/j.cattod.2013.10.088.

[18] B. Ohtani, K. Iwai, H. Kominami, T. Matsuura, Y. Kera, S. Nishimoto, Titanium(IV) oxide photocatalyst of ultra-high activity for selective N-cyclization of an amino acid in aqueous suspensions, Chem. Phys. Lett. 242 (1995) 315–319. doi:10.1016/0009-2614(95)00740-U.

[19] P.K.J. Robertson, J.M.C. Robertson, D.W. Bahnemann, Removal of microorganisms and their chemical metabolites from water using semiconductor photocatalysis, J. Hazard. Mater. 211-212 (2012) 161–171. doi:10.1016/j.jhazmat.2011.11.058.

[20] X. Lan, L. Wang, B. Zhang, B. Tian, J. Zhang, Preparation of lanthanum and boron co-doped TiO_2 by modified sol–gel method and study their photocatalytic activity, Catal. Today. 224 (2014) 163–170. doi:10.1016/j.cattod.2013.10.062.

[21] Y. Chen, K. Liu, Preparation of granulated N-doped TiO_2 / diatomite composite

ACCEPTED MANUSCRIPT

and its applications of visible light degradation and disinfection, Powder Technol. 303 (2016) 176–191. doi:10.1016/j.powtec.2016.09.038.

[22] J. Li, X. Yang, X. Yu, L. Xu, W. Kang, W. Yan, et al., Rare earth oxide-doped titania nanocomposites with enhanced photocatalytic activity towards the degradation of partially hydrolysis polyacrylamide, Appl. Surf. Sci. 255 (2009) 3731–3738. doi:10.1016/j.apsusc.2008.10.029.

[23] F. Wu, W. Liu, J. Qiu, J. Li, W. Zhou, Y. Fang, et al., Enhanced photocatalytic degradation and adsorption of methylene blue via TiO_2 nanocrystals supported on graphene-like bamboo charcoal, Appl. Surf. Sci. (2015). doi:10.1016/j.apsusc.2015.08.161.

[24] N.P. Radhika, R. Selvin, R. Kakkar, A. Umar, Recent advances in nano-photocatalysts for organic synthesis, Arab. J. Chem. (2016). doi:10.1016/j.arabjc.2016.07.007.

[25] T.-D. Nguyen-Phan, V.H. Pham, E.W. Shin, H.-D. Pham, S. Kim, J.S. Chung, et al., The role of graphene oxide content on the adsorption-enhanced photocatalysis of titanium dioxide/graphene oxide composites, Chem. Eng. J. 170 (2011) 226–232. doi:10.1016/j.cej.2011.03.060.

[26] X. Li, R. Shen, S. Ma, X. Chen, J. Xie, Graphene-based heterojunction photocatalysts, Appl. Surf. Sci. 430 (2018) 53–107. doi:10.1016/j.apsusc.2017.08.194.

[27] X. Li, J. Yu, S. Wageh, A.A. Al-Ghamdi, J. Xie, Graphene in Photocatalysis: A Review, Small. 12 (2016) 6640–6696. doi:10.1002/smll.201600382.

[28] Y. YU, G. CHEN, Y. ZHOU, Z. HAN, Recent advances in rare-earth elements modification of inorganic semiconductor-based photocatalysts for efficient solar energy conversion: A review, J. Rare Earths. 33 (2015) 453–462.

ACCEPTED MANUSCRIPT

doi:10.1016/S1002-0721(14)60440-3.

[29] L. Yu, X. Yang, J. He, Y. He, D. Wang, Synthesis of magnetically separable N, La-doped TiO_2 with enhanced photocatalytic activity, Sep. Purif. Technol. 144 (2015) 107–113. doi:10.1016/j.seppur.2015.02.007.

[30] Y. Zhang, H. Xu, Y. Xu, H. Zhang, Y. Wang, The effect of lanthanide on the degradation of RB in nanocrystalline Ln/TiO_2 aqueous solution, J. Photochem. Photobiol. A Chem. 170 (2005) 279–285. doi:10.1016/j.jphotochem.2004.08.001.

[31] V.Z. Baldissarelli, T. de Souza, L. Andrade, L.F.C. de Oliveira, K.J. José, R. de F.P.M. Moreira, Preparation and photocatalytic activity of TiO_2-exfoliated graphite oxide composite using an ecofriendly graphite oxidation method, Appl. Surf. Sci. 359 (2015) 868–874. doi:10.1016/j.apsusc.2015.10.199.

[32] Z.M. El-Bahy, A.A. Ismail, R.M. Mohamed, Enhancement of titania by doping rare earth for photodegradation of organic dye (Direct Blue)., J. Hazard. Mater. 166 (2009) 138–43. doi:10.1016/j.jhazmat.2008.11.022.

[33] V. Štengl, S. Bakardjieva, N. Murafa, Preparation and photocatalytic activity of rare earth doped TiO_2 nanoparticles, Mater. Chem. Phys. 114 (2009) 217–226. doi:10.1016/j.matchemphys.2008.09.025.

[34] Y. Min, K. Zhang, W. Zhao, F. Zheng, Y. Chen, Y. Zhang, Enhanced chemical interaction between TiO_2 and graphene oxide for photocatalytic decolorization of methylene blue, Chem. Eng. J. 193-194 (2012) 203–210. doi:10.1016/j.cej.2012.04.047.

[35] C. Liu, L. Zhang, R. Liu, Z. Gao, X. Yang, Z. Tu, et al., Hydrothermal synthesis of N-doped TiO_2 nanowires and N-doped graphene heterostructures with enhanced photocatalytic properties, J. Alloys Compd. 656 (2016) 24–32. doi:10.1016/j.jallcom.2015.09.211.

ACCEPTED MANUSCRIPT

[36] J. Suave, S.M. Amorim, J. Ângelo, L. Andrade, A. Mendes, R.F.P.M. Moreira, TiO_2/reduced graphene oxide composites for photocatalytic degradation in aqueous and gaseous medium, J. Photochem. Photobiol. A Chem. 348 (2017) 326–336. doi:10.1016/j.jphotochem.2017.08.064.

[37] V. Binas, D. Venieri, D. Kotzias, G. Kiriakidis, Modi fi ed TiO_2 based photocatalysts for improved air and health quality, J Mater. 3 (2017) 3–16. doi:10.1016/j.jmat.2016.11.002.

[38] Y. Ao, L. Xu, P. Wang, C. Wang, J. Hou, J. Qian, et al., Graphene and TiO_2 co-modified flower-like $Bi_2O_2CO_3$: A novel multi-heterojunction photocatalyst with enhanced photocatalytic activity, Appl. Surf. Sci. 355 (2015) 411–418. doi:10.1016/j.apsusc.2015.07.027.

[39] C. P. Kumar, N. O. Gopal, T. C. Wang, M. S. Wong, S. C. Ke, EPR Investigation of TiO_2 Nanoparticles with Temperature-Dependent Properties, The Journal of Physical Chemistry B, 110 (2006) 5223-5229, doi: 10.1021/jp057053t.

[40] O. I. Micic, Y. Zhang, K. R. Cromack, A. D. Trifunac, M. C. Thurnauer. Trapped Holes on TiO_2 Colloids Studied by Electron Paramagnetic Resonance, The Journal of Physical Chemistry, 97 (1993) 7277-7283. doi: 10.1021/j100130a026

[41] S. Silvestri, L. Szpoganicz, J. Schultz, A. S. Mangrich, D. Hotza,D. E. García, J. A. Labrincha, Doped and undoped anatase-based plates obtained from paper templates for photocatalytic oxidation of NO_X, Ceramics International, 42 (2016) 12074-12083. doi: 10.1016/j.ceramint.2016.04.137

[42] J. Hongquan, L. Yanduo, L. Jingshen, W. Haiyan, W. Synergetic effects of lanthanum, nitrogen and phosphorus tri-doping on visiblelight photoactivity of TiO_2 fabricated by microwave-hydrothermal process, Journal of Rare Earths, 34 (2016) 604-613. doi: 10.1016/S1002-0721(16)60068-6.

ACCEPTED MANUSCRIPT

[43] A. J. Maira,K. L. Yeung, J. Soria, J. M. Coronad, C. Belver, C. Y. Lee, V. Augugliaro, Gas-phase photo-oxidation of toluene using nanometer-size TiO_2 catalysts, Applied Catalysis B: Environmental, 29 (2001) 327-336, doi: 10.1016/S0926-3373(00)00211-3.

[44] U. Alam, M. Fleisch, I. Kretschmer, D. Bahnemann, M. Muneer, M. One-step hydrothermal synthesis of Bi-TiO_2 nanotube/graphene composites: An efficient photocatalyst for spectacular degradation of organic pollutants under visible light irradiation, Applied Catalysis B: Environmental, 218 (2017) 758-769, doi: 10.1016/j.apcatb.2017.06.016.

[45] E. A. Konstantinova, V. Y. Gayvoronskiy, V. Y. Timoshenko, P. K. Kashkarov, Study of Spin Centers in Nanocrystalline Titanium Dioxide with a High Degree of Photocatalytic Activity, Semiconductors, 44 (2010) 1059-1063, doi: 10.1134/S106378261008018X.

[46] C. P. Sibu, S. R. Kumar, P. Mukundan, K. G. K. Warrier, Structural Modifications and Associated Properties of Lanthanum Oxide Doped Sol-Gel Nanosized Titanium Oxide, Chemistry of Materials, 14 (2002) 2876-2881, doi: 10.1021/cm010966p.

[47] D. Xu, L. Feng, A. Lu, Characterizations of lanthanum trivalent ions/TiO_2 nanopowders catalysis prepared by plasma spray, Journal of Colloid and Interface Science, 329 (2009) 395-403, doi: 10.1016/j.jcis.2008.09.048.

[48] K.M. Parida, N. Sahu, Visible light induced photocatalytic activity of rare earth titania nanocomposites, J. Mol. Catal. A Chem. 287 (2008) 151–158. doi:10.1016/j.molcata.2008.02.028.

[49] S. Yuan, Q. Sheng, J. Zhang, F. Chen, Synthesis of La^{3+} doped mesoporous titania with highly crystallized walls, Microporous Mesoporous Mater. 79 (2005) 93–99. doi:10.1016/j.micromeso.2004.10.028.

ACCEPTED MANUSCRIPT

[50] L. Elsellami, H. Lachheb, A. Houas, Synthesis, characterization and photocatalytic activity of Li-, Cd-, and La-doped TiO_2, Mater. Sci. Semicond. Process. 36 (2015) 103–114. doi:10.1016/j.mssp.2015.03.032.

ACCEPTED MANUSCRIPT